

Functional characterization of 12 dihydropyrimidinase allelic variants in Japanese individuals for the prediction of 5-fluorouracil treatment-related toxicity

Eiji HISHINUMA, Yoko NARITA, Evelyn Marie GUTIÉRREZ RICO, Akiko UEDA,
Kai OBUCHI, Yoshikazu TANAKA, Sakae SAITO, Shu TADAKA, Kengo
KINOSHITA, Masamitsu MAEKAWA, Nariyasu MANO, Tomoki NAKAYOSHI,
Akifumi ODA, Noriyasu HIRASAWA, Masahiro HIRATSUKA

Advanced Research Center for Innovations in Next-Generation Medicine, Tohoku
University, Sendai, 980-8573, Japan (E.H., A.U., Y.T., S.S., K.K., M.M., N.H., M.H.)

Laboratory of Pharmacotherapy of Life-Style Related Diseases, Graduate School of
Pharmaceutical Sciences, Tohoku University, Sendai 980-8578, Japan (Y.N., E.M.G.R.,
K.O., N.H., M.H.)

Tohoku Medical Megabank Organization, Tohoku University, Sendai, 980-8573, Japan
(E.H., S.S., S.T., K.K., M.H.)

Graduate School of Life Sciences, Tohoku University, Sendai, 980-8577, Japan (Y.T.)

Graduate School of Information Sciences, Tohoku University, Sendai, 980-8579, Japan
(K.K.)

Department of Pharmaceutical Sciences, Tohoku University Hospital, Sendai 980-8574,
Japan (M.M., N.M., N.H., M.H.)

Department of Biophysical Chemistry, Faculty of Pharmacy, Meijo University, Nagoya
468-8503, Japan (T.N., A.O.)

Graduate School of Information Sciences, Hiroshima City University, Hiroshima 731-
3194, Japan (T.N.)

Running title: Functional characterization of 12 DHPase allelic variants

Corresponding author:

Dr. Masahiro Hiratsuka, Ph.D.

Laboratory of Pharmacotherapy of Life-Style Related Diseases, Graduate School of
Pharmaceutical Sciences, Tohoku University, 6-3, Aoba, Aramaki, Aoba-ku, Sendai,
980-8578, Japan

Tel & Fax: +81-22-717-7049

E-mail: masahiro.hiratsuka.a8@tohoku.ac.jp

Number of text pages: 35

Number of tables: 4

Number of figures: 7

Number of references: 37

Number of words in Abstract: 247

Number of words in Introduction: 854

Number of words in Discussion: 1244

Abbreviations: 5-FU, 5-fluorouracil; β -UP, β -ureidopropionase; bUPA, β -ureidopropionic acid; CL_{int} , intrinsic clearance; DHPase, dihydropyrimidinase; DPD, dihydropyrimidine dehydrogenase; DTT, dithiothreitol; FUH₂, dihydro-5-fluorouracil; FUPA, fluoro- β -ureidopropionic acid; K_m , Michaelis constant; LC-MS/MS, liquid chromatography-tandem mass spectrometry; SNV, single nucleotide variant; ToMMo, Tohoku Medical Megabank Organization; UH₂, dihydrouracil; V_{max} , maximum velocity; WGS, whole-genome sequences.

Abstract

The drug 5-fluorouracil (5-FU) is the first-choice chemotherapeutic agent against advanced-stage cancers. However, 10–30% of treated patients experience grade 3–4 toxicity. The deficiency of dihydropyrimidinase (DHPase), which catalyzes the second step of the 5-FU degradation pathway, is correlated with the risk of developing toxicity. Thus, genetic polymorphisms within *DPYS*, the DHPase-encoding gene, could potentially serve as predictors of severe 5-FU-related toxicity. We identified 12 novel *DPYS* variants in 3,554 Japanese individuals, but the effects of these mutations on function remain unknown. In the current study, we performed *in vitro* enzymatic analyses of the 12 newly identified DHPase variants. Dihydrouracil or dihydro-5-FU hydrolytic ring-opening kinetic parameters, K_m and V_{max} , and intrinsic clearance ($CL_{int} = V_{max}/K_m$) of the wild-type DHPase and eight variants were measured. Five of these variants (R118Q, H295R, T418I, Y448H, and T513A) showed significantly reduced CL_{int} compared with that in the wild-type. The parameters for the remaining four variants (V59F, D81H, T136M, and R490H) could not be determined as dihydrouracil and dihydro-5-FU hydrolytic ring-opening activity was undetectable. We also determined DHPase variant protein stability using cycloheximide and bortezomib. The mechanism underlying the observed changes in the kinetic parameters was clarified

using blue-native polyacrylamide gel electrophoresis and three-dimensional structural modeling. The results suggested that the decrease or loss of DHPase enzymatic activity was due to reduced stability and oligomerization of DHPase variant proteins. Our findings support the use of *DPYS* polymorphisms as novel pharmacogenomic markers for predicting severe 5-FU-related toxicity in the Japanese population.

Significance Statement

DHPase contributes to the degradation of 5-fluorouracil, and genetic polymorphisms that cause decreased activity of DHPase can cause severe toxicity. In this study, we performed functional analysis of 12 DHPase variants in the Japanese population and identified 9 genetic polymorphisms that cause reduced DHPase function. In addition, we found that the ability to oligomerize and the conformation of the active site are important for the enzymatic activity of DHPase.

Introduction

The drug 5-fluorouracil (5-FU) is used in chemotherapy for various forms of cancer, including those presenting with solid tumors in the gastrointestinal tract, breast, head, and neck (Wigmore et al., 2010; Kobuchi and Ito, 2020). It is an antimetabolite that works by preventing cell proliferation and is used in combination with other agents or as a single-drug treatment (Wigmore et al., 2010). However, despite over 40 years of clinical use and optimization of administration methods, the response rate remains low because of the development of chemoresistance (Lokich, 1998; Vodenkova et al., 2020). Moreover, a significant number of patients (10–30%) develop symptoms from toxicity caused by 5-FU, such as mucositis, diarrhea, neutropenia, thrombocytopenia, and hand-foot syndrome (Lokich, 1998; Kunicka et al., 2016; Vodenkova et al., 2020). Thus, predictive biomarkers for toxicity remain an important focus of future research, as severe toxicity might lead not only to treatment interruption but also to patient death (Kunicka et al., 2016; Vodenkova et al., 2020).

Once the agent reaches the circulatory system, most of the administered 5-FU (more than 80%) is metabolized to dihydro-5-FU (FUH₂) in the liver by the enzyme dihydropyrimidine dehydrogenase (DPD; EC 1.3.1.2). (Heggie et al., 1987; Kunicka et al., 2016; Kobuchi and Ito, 2020). Dihydropyrimidinase (DHPase; EC 3.5.2.2) then

catalyzes the hydrolytic ring opening of FUH₂. Finally, the resulting fluoro-β-ureidopropionic acid (FUPA) is hydrolyzed to fluoro-β-alanine by β-ureidopropionase (β-UP, EC 3.5.1.6). In Caucasians, genetic polymorphisms in *DPYD*, the gene encoding DPD, contribute to individual differences in 5-FU toxicity, and the Clinical Pharmacogenetics Implementation Consortium (CPIC) guidelines have already been established for dose adjustment based on four risk variants (*DPYD*2A*, *DPYD*13*, c.2846A>T, and c.1129-5923C>G/hapB3) (Amstutz et al., 2018). However, these polymorphisms have not been identified in Asian populations (van Kuilenburg, 2004; Maekawa et al., 2007; Hishinuma et al., 2018; Yokoi et al., 2020; Hishinuma et al., 2022). Toxicity associated with 5-FU has also been observed in cancer patients with regular DPD enzymatic activity, suggesting a potential deficiency of DHPase, the second enzyme in the pyrimidine degradation pathway. Reduced enzymatic activity of DHPase causes FUH₂ to accumulate in the blood, which is reversibly converted to 5-FU by the activity of DPD, resulting in severe 5-FU-related toxicity (Shiotani and Weber, 1981).

The human DHPase-encoding gene, *DPYS*, is located on chromosome 8q22, consists of 10 exons, and features a 1,560-bp open reading frame, encoding a polypeptide containing 519 amino acid residues (Hamajima et al., 1998; van Kuilenburg

et al., 2006). DHPase deficiency is an autosomal recessive condition characterized by dihydropyrimidinuria (Duran et al., 1991). The clinical phenotype of DHPase-deficient patients is highly variable; while asymptomatic patients have been identified, symptoms can range from early infantile-onset of severe neurological involvement to dysmorphic features, including feeding problems and late-onset mild intellectual disability (Ohba et al., 1994; van Gennip et al., 1994; Hayashi et al., 1996; van Gennip et al., 1997; Sumi et al., 1998; van Kuilenburg et al., 2007; van Kuilenburg et al., 2010; Yeung et al., 2013). Previously, we reported a Japanese patient with severe capecitabine-related toxicity associated with DHPase deficiency due to a compound heterozygous mutation in the *DPYS* gene causing two enzyme loss of function mutations, c.1001A>G (p.Q334R) and c.1393C>T (p.R465X) (Hiratsuka et al., 2015). Nakajima et al. identified eight variants, including four with novel missense mutations (c.750G>A [p.M250I], c.884A>G [p.H295R], c.1253C>T [p.T418I], and c.1469G>A [p.R490H]) and one with a novel deletion (c.210delG), in four Asian patients diagnosed with DHPase deficiency (Nakajima et al., 2017). Notably, the identification of these DHPase-deficient patients can be attributed to recently enhanced diagnostic efforts in Asian populations (Akai et al., 2015; Nakajima et al., 2016). Thus, *DPYS* polymorphisms could become essential in predicting 5-FU-related toxicity in patients, including those from Asian populations.

We previously described the functional characterization of 21 DHPase variants that have been identified in various ethnic groups (Hishinuma et al., 2017; Hishinuma et al., 2020). Most of these variants may contribute to the large interindividual variability in the pharmacokinetics and pharmacodynamics of 5-FU. The *DPYS* polymorphism, like the *DPYD* polymorphism, may have large racial differences, necessitating detailed analysis for each population. Therefore, we extracted information on missense mutations of the *DPYS* gene from the whole-genome sequences (WGS) database of 3,554 Japanese individuals and identified 19 *DPYS* variants causing amino acid substitutions (Table 1) (Tadaka et al., 2021). Among these, the functional consequences of the alterations in 12 novel *DPYS* variants were unknown. Identifying variants that cause a significant decrease or loss of DHPase activity is important for predicting the development of severe toxicity caused by 5-FU.

In the current study, we aimed to characterize the enzymatic activity of the wild-type DHPase and the 12 DHPase variants using recombinant proteins expressed in 293FT cells and determine the kinetic parameters of these variant enzymes using assays for the dihydrouracil (UH₂) and FUH₂ hydrolytic ring-opening activities. We also evaluated DHPase variant protein stability by adding cycloheximide or bortezomib to the transfected cells and further clarified the enzymatic reduction using blue-native

polyacrylamide gel electrophoresis (PAGE) and three-dimensional (3D) structural modeling. Our results indicate the potential suitability of *DPYS* polymorphisms as novel pharmacogenomic markers in predicting severe 5-FU-related toxicity in the Japanese population.

Materials and methods

Chemicals and reagents

Antibodies were purchased from the following commercial sources: polyclonal anti-human DHPase antibody (Ab205039), Abcam (Cambridge, MA, USA); polyclonal anti-human DHPase antibody (LS-C80425), LifeSpan BioSciences (Seattle, WA, USA). Other chemicals and reagents were the same as in previous reports (Hishinuma et al., 2017).

Sanger sequencing

Genomic DNA was isolated from the whole blood of participating Japanese subjects of the cohort study conducted by the Tohoku Medical Megabank Organization (ToMMo) (Kuriyama et al., 2016; Minegishi et al., 2019; Hozawa et al., 2021). Informed consent was obtained from all research participants, and the study was approved by the Tohoku Medical Megabank Organization ethics committee (permission numbers 2017-4-26, 2017-4-58, and 2017-4-090) and the Tohoku University Graduate School of Pharmaceutical Sciences ethics committee (permission number 14-08). *DPYS* sequence alterations were identified using Sanger sequencing according to previously described methods (Akai et al., 2015; Hishinuma et al., 2018; Hishinuma et al., 2022).

The primer pairs used to detect single nucleotide variants (SNVs) in Sanger sequencing are listed in Table 2.

cDNA cloning and construction of expression vectors

Expression vectors, pcDNA3.4 (Thermo Fisher Scientific, Waltham, MA, USA) containing the wild-type human *DPYS* or the 12 variant cDNAs were prepared as previously described (Hishinuma et al., 2017).

DHPase variant expression in 293FT cells

The 293FT cells derived from human embryonic kidney cells were seeded at a density of 2.0×10^6 cells/10-cm dish. After 24 h, cells were transfected with plasmids carrying *DPYS* cDNAs (5 μ g each) using TransFectin lipid reagent (Bio-Rad Laboratories, Hercules, CA, USA). S-9 fractions and His-DHPase protein were prepared as previously described (Hishinuma et al., 2017).

Determination of DHPase protein expression through immunoblotting following sodium dodecyl sulfate (SDS)-PAGE

Proteins were separated using SDS-PAGE, and immunoblotting was performed as previously described (Hishinuma et al., 2017). The concentration of S-9 fraction protein was quantified by bicinchoninic acid assay, and 10 µg/lane of S-9 fractions were used for SDS-PAGE. DHPase was detected using a polyclonal anti-human DHPase antibody (1:2,000; LS-C80425) and HRP-conjugated goat anti-rabbit IgG (1:5,000). V59F was detected using a polyclonal anti-human DHPase antibody (1:2,000; Ab205039) and HRP-conjugated goat anti-rabbit IgG (1:5,000). GAPDH antibody was used as a loading control (1:5,000), and HRP-conjugated goat anti-rabbit IgG (1:10000) was used as the secondary antibody. DHPase expression levels were normalized to the GAPDH luminescence intensity.

Immunoblotting following blue-native PAGE

Immunoblotting following blue-native PAGE was performed as previously described (Hishinuma et al., 2017). DHPase was detected using a polyclonal anti-human DHPase antibody (1:2,000; Ab205039) and HRP-conjugated goat anti-rabbit IgG (1:5,000).

Gel filtration chromatography

The DHPase protein was filtered using a MILLEX-GV 0.22 μm filter (Merck, Darmstadt, Germany) after preparing the S-9 fraction. Gel filtration chromatography was performed using an AKTA-FPLC system (GE Healthcare, Tokyo, Japan). The buffer for gel filtration chromatography contained 20 mM Tris-HCl and 200 mM sodium chloride (pH 8.0), and Superdex200 10/300GL columns (1.0 \times 30 cm, 24 mL, GE Healthcare) were used for sample fractionation. The sample injection volume was 0.5 mL, and fractions were collected per 0.5 mL at a flow rate of 0.5 mL/min. The collected fractions were analyzed using immunoblotting after SDS-PAGE and blue-native PAGE to confirm the expression of DHPase and the presence of the DHPase oligomer, respectively.

A calibration curve was generated using standard proteins blue dextran (2,000 kDa), ferritin (440 kDa), aldolase (158 kDa), conalbumin (75 kDa), ovalbumin (44 kDa), carbonic anhydrase (29 kDa), and ribonuclease A (13.7 kDa). The K_{av} value was calculated from the elution volume of each protein, and the calibration curve was obtained by plotting the molecular weight against the K_{av} value. The elution volume of blue dextran was used as the void volume.

UH₂ and FUH₂ hydrolytic ring-opening assays

UH₂ or FUH₂ hydrolytic ring-opening assay was performed as previously described (Hishinuma et al., 2017). Briefly, UH₂ (0.3–300 μM) or FUH₂ (1–300 μM) was added to the DHPase protein (10 μg) and incubated at 37 °C for 10 min. The reactions were stopped by adding acetonitrile containing 1 μM FUPA or 10 μM bUPA as the internal standard.

After precipitating proteins by centrifugation at 14,000 × g for 5 min, the supernatant was vacuum-dried at 40 °C for 1.5 h and redissolved in 0.1% (v/v) formic acid in water. Samples were injected into a liquid chromatography-mass spectrometry (LC-MS) system (API5000 triple quadrupole mass spectrometer; SCIEX, Framingham, MA, USA). Using bUPA and FUPA metabolite standards, standard curves were constructed for concentrations ranging from 0.1 to 30 μM. The enzymatic activity was normalized to the corresponding DHPase expression levels determined by immunoblotting after SDS-PAGE.

Stability and degradation analysis of DHPase variants

The stability and degradation process of the DHPase variants was investigated as previously described (Hishinuma et al., 2017). After 24 h of transfection with *DPYS* variants, 293FT cells were incubated with 50 μg/mL cycloheximide for 24–48 h or 0.5

μM bortezomib for 24 h. DHPase proteins were evaluated using immunoblotting following SDS-PAGE. DHPase expression levels were normalized to the GAPDH luminescence intensity.

Statistical analysis

Michaelis constant (K_m), maximum velocity (V_{max}), and intrinsic clearance ($CL_{int} = V_{max}/K_m$) values were calculated using SigmaPlot 12.5 Enzyme Kinetics Module (Systat Software Inc., Chicago, USA). Each value was obtained in triplicate and expressed as mean \pm standard deviation. All assays and measurements were performed in triplicate using a single S-9 preparation. Statistical variance in protein expression and kinetic parameters was analyzed using IBM SPSS Statistics Ver. 22 (International Business Machines, Armonk, NY, USA). Differences or correlations with $P < 0.05$ were considered significant.

3D structural modeling of DHPase

A 3D structural modeling analysis of DHPase was performed as previously described (Hishinuma et al., 2017). Discovery Studio 4.5 was used for DHPase 3D imaging.

Results

Twelve novel *DPYS* allelic variants in Japanese participants were previously identified using WGS (Tadaka et al., 2021). Sanger sequencing was performed to validate these identified variants, and all exon SNV and WGS results were consistent with those obtained using Sanger sequencing (Table 1).

The wild-type DHPase and the 12 variant proteins were transiently expressed in 293FT cells. The truncated variant W117X was excluded from the study because we expected it to be inactive owing to alterations that affected its structural and enzymatic integrity. The DHPase expression levels were determined using quantitative immunoblotting after SDS-PAGE with a polyclonal DHPase antibody (LS-C80425), which recognizes the N-terminal region of the DHPase protein, thus detecting all DHPase variants except V59F (Fig. 1A). The V59F protein was detected using a different polyclonal DHPase antibody that recognizes the C-terminal region (Ab205039, Fig. 1B). The average levels of wild-type and variant DHPase proteins are shown in Fig. 1C. We normalized the DHPase protein levels equivalent to 1 μ g of His-DHPase as 1 DHPase unit. The DHPase unit levels of D81H, T136M, A189V, and T418I were significantly decreased ($P < 0.05$), and those of H365Y, R490H, and T513A were significantly increased ($P < 0.05$) compared with that of wild-type DHPase.

The kinetic parameters of UH₂ and FUH₂ hydrolytic ring opening by the DHPase variant are shown in Table 3 and 4, respectively. The Michaelis–Menten curves of DHPase variants are shown in Fig. 2A and 2B. The kinetic parameters could not be determined for four variants (V59F, D81H, T136M, and R490H) as no UH₂ and FUH₂ hydrolytic ring-opening activity was detected. The K_m , V_{max} , and CL_{int} values for the hydrolytic ring opening of UH₂ by wild-type DHPase were 8.32 μ M, 45.37 pmol/min/DHPase unit, and 5.45 μ L/min/DHPase unit, respectively. Compared with the wild-type DHPase, H295R showed a significantly lower K_m value ($P < 0.05$), whereas H365Y and G410S showed significantly higher V_{max} values ($P < 0.005$), and four variants (H295R, T418I, Y448H, and T513A) showed significantly lower V_{max} values ($P < 0.005$), whereas H295R showed a significantly lower CL_{int} value ($P < 0.005$). The K_m , V_{max} , and CL_{int} values for the hydrolytic ring opening of FUH₂ by wild-type DHPase were 43.01 μ M, 87.35 pmol/min/DHPase unit, and 2.03 μ L/min/DHPase unit, respectively. Compared with the wild-type DHPase, six variants (R118Q, A189V, H295R, T418I, Y448H, and T513A) showed significantly lower V_{max} values ($P < 0.005$), and five variants (R118Q, H295R, T418I, Y448H, and T513A) showed significantly lower CL_{int} values ($P < 0.005$). Moreover, the CL_{int} values for UH₂ and

FUH₂ hydrolytic ring opening (Fig. 3C) showed a significant correlation ($r^2 = 0.8916$, $P < 0.001$).

Immunoblotting after blue-native PAGE showed high-molecular-weight signal bands corresponding to the oligomeric forms of wild-type DHPase, H365Y, and G410S (Fig. 3). Conversely, no high-molecular-weight bands were detected for V59F, D81H, T136M, H295R, and R490H, whereas low-molecular-weight bands corresponding to monomeric DHPase were detected for D81H, T136M, H295R, and R490H. Both the high- and low-molecular-weight bands were detected for R118Q, A189V, T418I, Y448H, and T513A.

To calculate the molecular weight of the DHPase oligomer, gel filtration chromatography was performed using S-9 fractions containing wild-type DHPase and R490H (Fig. 4A). In SDS-PAGE, the DHPase proteins were observed in the fractions with elution volumes of 11.2 to 15.2 mL and 12.7 to 15.2 mL for wild-type DHPase and R490H, respectively. In contrast, an oligomeric band was observed in the fraction with an elution volume of 11.7 to 14.2 mL, and a monomeric band was observed in the fraction with an elution volume of 13.7 to 14.7 mL in blue-native PAGE. Next, we plotted the DHPase protein expression against the elution volume of the DHPase protein and the absorbance at 280 nm wavelength against the elution volume of the standard

protein (Fig. 4B). The 11.2 mL fraction contained proteins with molecular weights of 158–440 kDa, and the 13.7 mL fraction contained proteins with molecular weights of 44–158 kDa. Linearity was obtained for the K_{av} values and molecular weights of the standard proteins (Fig. 4C).

To evaluate the *in vitro* stability of the DHPase variant protein, cycloheximide, an inhibitor of eukaryotic protein synthesis, was added after the transfection of 293FT cells with the *DPYS* expression plasmid. DHPase protein levels were determined using immunoblotting on samples collected after 0, 24, and 48 h of cycloheximide treatment (Fig. 5A). The expression of the wild-type protein and 10 DHPase variants (D81H, R118Q, A189V, H295R, H365Y, G410S, T418I, T448H, R490H, and T513A) remained constant up to 48 h, whereas V59F and T136M showed significant decreases in expression at 24 and 48 h ($P < 0.01$).

To assess the structural stability of the DHPase variant proteins in relation to proteasome-mediated degradation, we treated 293FT cells with bortezomib, a 26S proteasome inhibitor, after 24 h of transfection. DHPase protein levels were determined using immunoblotting on samples collected after 24 h of bortezomib treatment (Fig. 5B). Bortezomib treatment increased the protein levels of V59F, indicating that the proteasome system is involved in the degradation of V59F.

Close-up views of the 3D models for the crystal protein structure of V59F, D81H, T136M, and H295R mutation sites are shown in Fig. 6A, 6B, 6C, and 6D, respectively. The V59F substitution variant formed π -alkyl interactions between I395 and I403 and lacked the carbon-hydrogen bond between D17 and R394. The D81H substitution variant lacked the carbon-hydrogen bond between R78 and S79. The T136M substitution variant formed an alkyl interaction with Y168. In the H295R substitution variant, interactions among R295, M297, and L301 were observed, resulting in π - π interactions between Y164 and H192 through G298. Close-up views of the R118Q, T418I, and Y448H mutation sites are shown in Fig. 7A, 7B, and 7C, respectively. The R118Q substitution variant lacked a charge interaction with E115 and formed hydrogen bonds between F72 and F74 and π -alkyl interactions between I103 and Y168 through W117. The T418I substitution variant had a hydrogen bond between H419 and Q421 and carbon-hydrogen interactions between P73 and S77 through Q71 and D81.

Discussion

DHPase deficiency can lead to severe adverse effects during 5-FU-based treatment. Since DHPase deficiency is commonly reported in Asian populations, functional analysis of low-frequency SNVs contained in variant DHPase is essential for predicting 5-FU toxicity, especially in the Japanese population (Hiratsuka et al., 2015; Hishinuma et al., 2017; Nakajima et al., 2017). Therefore, in this study, we characterized the enzymatic activity of wild-type and 12 non-synonymous DHPase variants previously identified in 3,554 Japanese individuals and determined the kinetic parameters of these variant enzymes. The kinetic parameters of four variants (V59F, D81H, T136M, and R490H) could not be determined as their respective metabolites were below the quantification limit at the highest substrate concentration used. Significant alterations in expression levels were observed for several DHPase variants; the expression levels of recombinant proteins might be affected by a number of factors, including transfection deficiency, coding SNVs in transcriptional regulatory factors, coding SNVs in linkage disequilibrium with other SNVs that may have regulatory effects, and coding SNVs having codon usage preferences. Therefore, it is unclear whether these variants are differentially expressed among human individuals, and future studies are needed to elucidate the changes in their expression levels *in vivo*.

Previously, we reported a method for blue-native PAGE analysis to determine the non-denatured state of the protein and the close relationship between the band patterns of blue-native PAGE and CL_{int} values of DHPase variants (Hishinuma et al., 2017). In this study, the DHPase variants (V59F, D81H, T136M, H295R, and R490H) that did not form oligomers showed a significant decrease or loss in enzymatic activity, indicating the importance of oligomerization for the enzymatic activity of DHPase. It is important to calculate the exact molecular weight of the DHPase oligomer because DHPase is reported to form tetramers. Therefore, we determined the exact molecular weight of the oligomeric band identified around 720 kDa by performing gel filtration chromatography on wild-type DHPase and R490H, which showed an oligomeric band and a monomeric band in blue-native PAGE, respectively. The wild-type DHPase oligomeric band showed a weight of 158–440 kDa (which is consistent with the predicted weight of the DHPase tetramer, 216 kDa); in contrast, the monomeric band of R490H had a molecular weight of 44–154 kDa. These results indicate that the DHPase oligomeric band corresponds to the DHPase tetramer, emphasizing the importance of tetramer formation for DHPase enzymatic activity.

We further found that five DHPase variants (V59F, D81H, T136M, H295R, and R490H) showed markedly reduced activity for UH_2 and FUH_2 hydrolytic ring opening,

revealing no high-molecular-weight bands corresponding to oligomeric DHPase upon immunoblotting after blue-native PAGE. Tzeng et al. reported that A13, D14, I31, K373, and T383 form hydrogen bonds at the dimer–dimer interface of *Thermus* sp. DHPase (Tzeng et al., 2016). D17, D18, L35, K384, and R394 are located around the oligomerization interaction site in human DHPase. Because D17 and R394 are in an oligomerization interaction site, the abolition of the carbon-hydrogen bond between D17 and R394 due to the V59F substitution could inhibit oligomerization. Collectively, oligomerization induced by interactions across each DHPase subunit is essential for DHPase activity in UH₂ and FUH₂ hydrolytic ring opening. Additionally, V59F showed a decrease in expression after the addition of cycloheximide and an increase in expression after the addition of bortezomib, suggesting that proteasome-mediated degradation contributes to the degradation of V59F protein when compared with that of wild-type. The conformational changes caused by the amino acid substitutions in the V59F variant could have led to protein misfolding and subsequent instability, resulting in the observed enzymatic inactivity.

Among the five variants V59F, D81H, T136M, H295R, and R490H, all except V59F lacked conformational changes at the oligomerization interaction sites. Hsieh et al. reported that in *Tetraodon nigroviridis* DHPase (*TnDhp*), two dynamic loops (A69-

R74 and M158-M165) containing the aromatic residues F70 and Y160 move closer to the active site, thus locking the substrates into the characteristic closed-form (Hsieh et al., 2013). In human DHPase, these two dynamic loops correspond to P73-R78 and M162-M169, which contain F74 and Y164, respectively. Nakajima et al. reported that structural rearrangements to accommodate the R295 side chain have detrimental effects on the geometry of the substrate-binding site (Nakajima et al., 2017). In these variants, amino acid substitutions led to conformational changes in the dynamic loops, which resulted in the reported enzymatic inactivity. T136M showed decreased expression following the addition of cycloheximide, but its degradation was not inhibited by bortezomib. The degradation observed in T136M may involve mechanisms other than the proteasome-mediated degradation system.

R490H, which is located on the C-terminal tail and extends toward another subunit in a swapping-like manner, is possibly involved in protein oligomerization. Hsieh et al. reported that the C-terminal tail-mediated dimerization of *TnDhp* might assist in opening the two dynamic loops for enzyme function (Hsieh et al., 2013). Nakajima et al. reported that an increase in C-terminal tail flexibility is likely to disturb dimer and oligomer association and thus, stability (Nakajima et al., 2017). We have also previously reported that R490C, in which enzymatic activity was practically eliminated,

showed no high-molecular-weight bands corresponding to oligomeric DHPase in immunoblotting after blue-native PAGE (Hishinuma et al., 2017). Taken together, the results suggest that R490H prevents oligomerization and markedly decreases DHPase activity.

The CL_{int} values for UH₂ and FUH₂ hydrolytic ring-opening assay regarding R118Q, T418I, Y448H, and T513A were 80–100% and 60–80%, respectively. For these variants, both high- and low-molecular-weight bands were detected in immunoblots after blue-native PAGE, confirming that both oligomeric and monomeric DHPase were formed. Nakajima et al. reported that an increase in sidechain hydrophobicity would make solvent exposure energetically less favorable and lead to minor structural rearrangements affecting enzymatic stability and activity (Nakajima et al., 2017).

The Y448H substitution had the effect of inducing a π - π interaction with F453 and a new connection with K88 via a π -alkyl interaction, causing a conformational change in the dynamic loop (P73-R78) on the extension of K88. The T513A substitution was located on the C-terminal tail and thus might have prevented oligomerization and reduced DHPase activity. For the A189V variant, although both the high- and low-molecular-weight bands were detected, the CL_{int} value was approximately 110% of the

wild-type DHPase. These results imply that the A189V variant shows regular enzymatic activity because of the increased activity of the A189V oligomers.

In conclusion, wild-type DHPase and 12 variants were expressed in 293FT cells, and their enzymatic activities were assessed *in vitro*. Among the 12 variants, 9 showed decreased enzymatic activity due to conformational changes in the active site or the interaction sites required for oligomerization. These variants may affect the pharmacokinetics of 5-FU and its oral prodrugs, leading to an increased risk of severe toxicity. There have been no reported cases of the development of 5-FU toxicity in patients with these variants, which may be attributable to the low allele frequencies of each *DPYS* polymorphism. However, it is possible that some patients are compound heterozygotes for these variant alleles, and their enzyme activities are expected to be analyzed in detail in the future. In addition, it is not known whether these mutations affect enzyme activity or oligomer formation *in vivo*, and more detailed *in vitro* and large-scale clinical studies are needed. These comprehensive findings provide insights into individual differences in 5-FU efficacy and toxicity due to differences in DHPase activity. They will facilitate further genotype-phenotype correlation studies and may provide the basis for dosage adjustment according to the *DPYS* genetic polymorphisms, similarly to the CPIC guidelines for the *DPYD* gene.

Acknowledgments

We thank the Biomedical Research Core at the Tohoku University Graduate School of Medicine for their technical support.

Authorship Contributions

Participated in research design: Hishinuma and Hiratsuka

Conducted experiments: Hishinuma, Narita, Gutiérrez Rico, Ueda, Obuchi, Saito, and
Maekawa

Contributed new reagents or analytic tools: Tanaka, Kinoshita, Maekawa, Mano,
Hirasawa, and Hiratsuka

Performed data analysis: Hishinuma, Narita, Saito, Tadaka, Nakayoshi, Oda, and
Hiratsuka

Wrote or contributed to the writing of the manuscript: Hishinuma, Narita, Gutiérrez
Rico, and Hiratsuka

References

- Akai F, Hosono H, Hirasawa N, and Hiratsuka M (2015) Novel single nucleotide polymorphisms of the dihydropyrimidinase gene (DPYS) in Japanese individuals. *Drug Metab Pharmacokinet* 30:127-129.
- Amstutz U, Henricks LM, Offer SM, Barbarino J, Schellens JHM, Swen JJ, Klein TE, McLeod HL, Caudle KE, Diasio RB, and Schwab M (2018) Clinical Pharmacogenetics Implementation Consortium (CPIC) Guideline for Dihydropyrimidine Dehydrogenase Genotype and Fluoropyrimidine Dosing: 2017 Update. *Clin Pharmacol Ther* 103:210-216.
- Duran M, Rovers P, de Bree PK, Schreuder CH, Beukenhorst H, Dorland L, and Berger R (1991) Dihydropyrimidinuria: a new inborn error of pyrimidine metabolism. *J Inher Metab Dis* 14:367-370.
- Hamajima N, Kouwaki M, Vreken P, Matsuda K, Sumi S, Imaeda M, Ohba S, Kidouchi K, Nonaka M, Sasaki M, Tamaki N, Endo Y, De Abreu R, Rotteveel J, van Kuilenburg A, van Gennip A, Togari H, and Wada Y (1998) Dihydropyrimidinase deficiency: structural organization, chromosomal localization, and mutation analysis of the human dihydropyrimidinase gene. *Am J Hum Genet* 63:717-726.
- Hayashi K, Kidouchi K, Sumi S, Mizokami M, Orito E, Kumada K, Ueda R, and Wada Y (1996) Possible prediction of adverse reactions to pyrimidine chemotherapy from urinary pyrimidine levels and a case of asymptomatic adult dihydropyrimidinuria. *Clin Cancer Res* 2:1937-1941.
- Heggie GD, Sommadossi JP, Cross DS, Huster WJ, and Diasio RB (1987) Clinical pharmacokinetics of 5-fluorouracil and its metabolites in plasma, urine, and bile. *Cancer Res* 47:2203-2206.
- Hiratsuka M, Yamashita H, Akai F, Hosono H, Hishinuma E, Hirasawa N, and Mori T (2015) Genetic polymorphisms of dihydropyrimidinase in a Japanese patient with capecitabine-induced toxicity. *PLoS One* 10:e0124818.
- Hishinuma E, Akai F, Narita Y, Maekawa M, Yamaguchi H, Mano N, Oda A, Hirasawa N, and Hiratsuka M (2017) Functional characterization of 21 allelic variants of dihydropyrimidinase. *Biochem Pharmacol* 143:118-128.
- Hishinuma E, Gutiérrez Rico E, and Hiratsuka M (2020) In Vitro Assessment of Fluoropyrimidine-Metabolizing Enzymes: Dihydropyrimidine Dehydrogenase, Dihydropyrimidinase, and β -Ureidopropionase. *J Clin Med* 9.
- Hishinuma E, Narita Y, Obuchi K, Ueda A, Saito S, Tadaka S, Kinoshita K, Maekawa M, Mano N, Hirasawa N, and Hiratsuka M (2022) Importance of Rare DPYD Genetic Polymorphisms for 5-Fluorouracil Therapy in the Japanese Population. *Front Pharmacol* 13:930470.
- Hishinuma E, Narita Y, Saito S, Maekawa M, Akai F, Nakanishi Y, Yasuda J, Nagasaki M, Yamamoto M, Yamaguchi H, Mano N, Hirasawa N, and Hiratsuka M (2018) Functional Characterization of 21

Allelic Variants of Dihydropyrimidine Dehydrogenase Identified in 1070 Japanese Individuals.
Drug Metab Dispos 46:1083-1090.

- Hozawa A, Tanno K, Nakaya N, Nakamura T, Tsuchiya N, Hirata T, Narita A, Kogure M, Nochioka K, Sasaki R, Takanashi N, Otsuka K, Sakata K, Kuriyama S, Kikuya M, Tanabe O, Sugawara J, Suzuki K, Suzuki Y, Kodama EN, Fuse N, Kiyomoto H, Tomita H, Uruno A, Hamanaka Y, Metoki H, Ishikuro M, Obara T, Kobayashi T, Kitatani K, Takai-Igarashi T, Ogishima S, Satoh M, Ohmomo H, Tsuboi A, Egawa S, Ishii T, Ito K, Ito S, Taki Y, Minegishi N, Ishii N, Nagasaki M, Igarashi K, Koshiba S, Shimizu R, Tamiya G, Nakayama K, Motohashi H, Yasuda J, Shimizu A, Hachiya T, Shiwa Y, Tominaga T, Tanaka H, Oyama K, Tanaka R, Kawame H, Fukushima A, Ishigaki Y, Tokutomi T, Osumi N, Kobayashi T, Nagami F, Hashizume H, Arai T, Kawaguchi Y, Higuchi S, Sakaida M, Endo R, Nishizuka S, Tsuji I, Hitomi J, Nakamura M, Ogasawara K, Yaegashi N, Kinoshita K, Kure S, Sakai A, Kobayashi S, Sobue K, Sasaki M, and Yamamoto M (2021) Study Profile of the Tohoku Medical Megabank Community-Based Cohort Study. *J Epidemiol* 31:65-76.
- Hsieh YC, Chen MC, Hsu CC, Chan SI, Yang YS, and Chen CJ (2013) Crystal structures of vertebrate dihydropyrimidinase and complexes from *Tetraodon nigroviridis* with lysine carbamylation: metal and structural requirements for post-translational modification and function. *J Biol Chem* 288:30645-30658.
- Kobuchi S and Ito Y (2020) Application of Pharmacometrics of 5-Fluorouracil to Personalized Medicine: A Tool for Predicting Pharmacokinetic-Pharmacodynamic/Toxicodynamic Responses. *Anticancer Res* 40:6585-6597.
- Kunicka T, Prochazka P, Krus I, Bendova P, Protivova M, Susova S, Hlavac V, Liska V, Novak P, Schneiderova M, Pitule P, Bruha J, Vycital O, Vodicka P, and Soucek P (2016) Molecular profile of 5-fluorouracil pathway genes in colorectal carcinoma. *BMC Cancer* 16:795.
- Kuriyama S, Yaegashi N, Nagami F, Arai T, Kawaguchi Y, Osumi N, Sakaida M, Suzuki Y, Nakayama K, Hashizume H, Tamiya G, Kawame H, Suzuki K, Hozawa A, Nakaya N, Kikuya M, Metoki H, Tsuji I, Fuse N, Kiyomoto H, Sugawara J, Tsuboi A, Egawa S, Ito K, Chida K, Ishii T, Tomita H, Taki Y, Minegishi N, Ishii N, Yasuda J, Igarashi K, Shimizu R, Nagasaki M, Koshiba S, Kinoshita K, Ogishima S, Takai-Igarashi T, Tominaga T, Tanabe O, Ohuchi N, Shimosegawa T, Kure S, Tanaka H, Ito S, Hitomi J, Tanno K, Nakamura M, Ogasawara K, Kobayashi S, Sakata K, Satoh M, Shimizu A, Sasaki M, Endo R, Sobue K, Tohoku Medical Megabank Project Study Group T, and Yamamoto M (2016) The Tohoku Medical Megabank Project: Design and Mission. *J Epidemiol* 26:493-511.
- Lokich J (1998) Infusional 5-FU: historical evolution, rationale, and clinical experience. *Oncology (Williston Park)* 12:19-22.

- Maekawa K, Saeki M, Saito Y, Ozawa S, Kurose K, Kaniwa N, Kawamoto M, Kamatani N, Kato K, Hamaguchi T, Yamada Y, Shirao K, Shimada Y, Muto M, Doi T, Ohtsu A, Yoshida T, Matsumura Y, Saijo N, and Sawada JI (2007) Genetic variations and haplotype structures of the DPYD gene encoding dihydropyrimidine dehydrogenase in Japanese and their ethnic differences. *J Hum Genet* 52:804-819.
- Minegishi N, Nishijima I, Nobukuni T, Kudo H, Ishida N, Terakawa T, Kumada K, Yamashita R, Katsuoka F, Ogishima S, Suzuki K, Sasaki M, Satoh M, Tohoku Medical Megabank Project Study G, and Yamamoto M (2019) Biobank Establishment and Sample Management in the Tohoku Medical Megabank Project. *Tohoku J Exp Med* 248:45-55.
- Nakajima Y, Meijer J, Dobritzsch D, Ito T, Zhang C, Wang X, Watanabe Y, Tashiro K, Meinsma R, Roelofsen J, Zoetekouw L, and van Kuilenburg ABP (2017) Dihydropyrimidinase deficiency in four East Asian patients due to novel and rare DPYS mutations affecting protein structural integrity and catalytic activity. *Mol Genet Metab* 122:216-222.
- Nakajima Y, Meijer J, Zhang C, Wang X, Kondo T, Ito T, Dobritzsch D, and Van Kuilenburg AB (2016) Altered Pre-mRNA Splicing Caused by a Novel Intronic Mutation c.1443+5G>A in the Dihydropyrimidinase (DPYS) Gene. *Int J Mol Sci* 17.
- Ohba S, Kidouchi K, Sumi S, Imaeda M, Takeda N, Yoshizumi H, Tatematsu A, Kodama K, Yamanaka K, Kobayashi M, and et al. (1994) Dihydropyrimidinuria: the first case in Japan. *Adv Exp Med Biol* 370:383-386.
- Shiotani T and Weber G (1981) Purification and properties of dihydrothymine dehydrogenase from rat liver. *J Biol Chem* 256:219-224.
- Sumi S, Imaeda M, Kidouchi K, Ohba S, Hamajima N, Kodama K, Togari H, and Wada Y (1998) Population and family studies of dihydropyrimidinuria: prevalence, inheritance mode, and risk of fluorouracil toxicity. *Am J Med Genet* 78:336-340.
- Tadaka S, Hishinuma E, Komaki S, Motoike IN, Kawashima J, Saigusa D, Inoue J, Takayama J, Okamura Y, Aoki Y, Shirota M, Otsuki A, Katsuoka F, Shimizu A, Tamiya G, Koshiha S, Sasaki M, Yamamoto M, and Kinoshita K (2021) jMorp updates in 2020: large enhancement of multi-omics data resources on the general Japanese population. *Nucleic Acids Res* 49:D536-d544.
- Thomas HR, Ezzeldin HH, Guarcello V, Mattison LK, Fridley BL, and Diasio RB (2007) Genetic regulation of dihydropyrimidinase and its possible implication in altered uracil catabolism. *Pharmacogenet Genomics* 17:973-987.
- Tzeng CT, Huang YH, and Huang CY (2016) Crystal structure of dihydropyrimidinase from *Pseudomonas aeruginosa* PAO1: Insights into the molecular basis of formation of a dimer. *Biochem Biophys Res Commun* 478:1449-1455.

- van Gennip AH, Abeling NG, Stroomer AE, van Lenthe H, and Bakker HD (1994) Clinical and biochemical findings in six patients with pyrimidine degradation defects. *J Inherit Metab Dis* 17:130-132.
- van Gennip AH, de Abreu RA, van Lenthe H, Bakkeren J, Rotteveel J, Vreken P, and van Kuilenburg AB (1997) Dihydropyrimidinase deficiency: confirmation of the enzyme defect in dihydropyrimidinuria. *J Inherit Metab Dis* 20:339-342.
- van Kuilenburg AB (2004) Dihydropyrimidine dehydrogenase and the efficacy and toxicity of 5-fluorouracil. *Eur J Cancer* 40:939-950.
- van Kuilenburg AB, Dobritzsch D, Meijer J, Meinsma R, Benoist JF, Assmann B, Schubert S, Hoffmann GF, Duran M, de Vries MC, Kurlemann G, Eyskens FJ, Greed L, Sass JO, Schwab KO, Sewell AC, Walter J, Hahn A, Zoetekouw L, Ribes A, Lind S, and Hennekam RC (2010) Dihydropyrimidinase deficiency: Phenotype, genotype and structural consequences in 17 patients. *Biochim Biophys Acta* 1802:639-648.
- van Kuilenburg AB, Meijer J, Dobritzsch D, Meinsma R, Duran M, Lohkamp B, Zoetekouw L, Abeling NG, van Tinteren HL, and Bosch AM (2007) Clinical, biochemical and genetic findings in two siblings with a dihydropyrimidinase deficiency. *Mol Genet Metab* 91:157-164.
- van Kuilenburg AB, van Lenthe H, and van Gennip AH (2006) Activity of pyrimidine degradation enzymes in normal tissues. *Nucleosides Nucleotides Nucleic Acids* 25:1211-1214.
- Vodenkova S, Buchler T, Cervena K, Veskrnova V, Vodicka P, and Vymetalkova V (2020) 5-fluorouracil and other fluoropyrimidines in colorectal cancer: Past, present and future. *Pharmacol Ther* 206:107447.
- Wigmore PM, Mustafa S, El-Beltagy M, Lyons L, Umka J, and Bennett G (2010) Effects of 5-FU. *Adv Exp Med Biol* 678:157-164.
- Yeung CW, Yau MM, Ma CK, Siu TS, Tam S, and Lam CW (2013) Diagnosis of dihydropyrimidinase deficiency in a Chinese boy with dihydropyrimidinuria. *Hong Kong Med J* 19:272-275.
- Yokoi K, Nakajima Y, Matsuoka H, Shinkai Y, Ishihara T, Maeda Y, Kato T, Katsuno H, Masumori K, Kawada K, Yoshikawa T, Ito T, and Kurahashi H (2020) Impact of DPYD, DPYS, and UPB1 gene variations on severe drug-related toxicity in patients with cancer. *Cancer Sci* 111:3359-3366.

Footnotes:

M.H. was supported by grants from the Japan Agency for Medical Research and Development (AMED) (grant no. JP19kk0305009), Takahashi Industrial and Economic Research Foundation, and Smoking Research Foundation. S.S., S.T., and K.K. were supported by grants from AMED (grant no. JP17km0105001 and JP21tm0124005). This research was also supported in part by the Tohoku Medical Megabank Project: Promoting Public Utilization of Advanced Research Infrastructure, and the Sharing and Administrative Network for Research Equipment funded by the Ministry of Education, Culture, Sports, Science, and Technology (MEXT). S.T. and K.K. were supported by grants for the Facilitation of R&D Platform for AMED Genome Medicine Support from AMED (grant no. JP20km0405001).

Competing interests

The authors declare no conflict of interest.

Figure legends

Figure 1. Expression of the wild-type and variant dihydropyrimidinase (DHPase) proteins. (A) DHPase protein levels were determined using immunoblotting following sodium dodecyl sulfate-polyacrylamide gel electrophoresis (SDS-PAGE). (B) The V59F protein was detected using a polyclonal DHPase antibody. (C) Unit levels of DHPase variants expressed in 293FT cells. Each bar represents the mean \pm standard deviation of three independent assays. * $P < 0.05$ compared with wild-type DHPase.

Figure 2. Michaelis–Menten curves of dihydropyrimidinase (DHPase) variants. The kinetic parameters K_m , V_{max} , and CL_{int} of (A) dihydrouracil and (B) dihydro-5-fluorouracil hydrolytic ring opening were determined. (C) Correlation between the CL_{int} ratios (relative to wild-type DHPase) for hydrolytic ring opening of dihydrouracil and dihydro-5-fluorouracil among DHPase variants. The CL_{int} ratios for the hydrolytic ring opening of dihydro-5-fluorouracil and dihydrouracil are plotted on the horizontal and vertical axes, respectively.

Figure 3. Immunoblotting after blue-native PAGE showing immunoreactive dihydropyrimidinase (DHPase) variant proteins. S-9 fractions of DHPase variant proteins were loaded into each lane in triplicate.

Figure 4. Gel filtration chromatographic analysis. (A) Dihydropyrimidinase (DHPase) protein levels were determined through immunoblotting following sodium dodecyl sulfate-polyacrylamide gel electrophoresis (SDS-PAGE) and blue-native PAGE. (B) DHPase protein levels of the fractions collected are shown in orange (wild-type) and green (R490H) lines; the black lines refer to the absorbance of the eluting marker proteins at 280 nm wavelength: ferritin (440 kDa), aldolase (158 kDa), conalbumin (75 kDa), ovalbumin (44 kDa), carbonic anhydrase (29 kDa), and ribonuclease A (13.7 kDa). (C) The column was calibrated with the marker proteins. The K_{av} values for the standard proteins and DHPase were calculated from the equation: $K_{av} = (V_e - V_o)/(V_c - V_o)$, where V_o is the void volume, V_e is the elution volume, and V_c is the column volume. A standard linear regression curve was generated by plotting the log of the molecular mass of the calibration proteins against their K_{av} values.

Figure 5. Stability of dihydropyrimidinase (DHPase) variant proteins *in vitro*. DHPase protein levels were determined using immunoblotting after sodium dodecyl sulfate-polyacrylamide gel electrophoresis (SDS-PAGE). Bars represent the mean \pm standard deviation of three independent assays. DHPase expression levels were normalized to the GAPDH luminescence intensity. (A) DHPase expression after cycloheximide treatment. $*P < 0.01$ compared with the result for 0 h for each variant. (B) DHPase expression after proteasome inhibition. $*P < 0.05$ compared with control for each variant.

Figure 6. Dihydropyrimidinase (DHPase) structural analysis. (A) Diagrams of a fragment of the crystal structures of wild-type DHPase (left panel) and V59F (right panel). The V59 and F59 residues are shown in yellow. The residues located in the oligomerization interaction site are colored in cyan. (B) Diagrams of a fragment of the crystal structures of wild-type DHPase. The D81 residue is shown in yellow. (C) Diagrams of a fragment of the crystal structures of T136M. The M136 residue is shown in yellow. (D) Diagrams of a fragment of the crystal structures of wild-type DHPase (left panel) and H295R (right panel). H295 and R295 are shown in yellow.

Figure 7. Dihydropyrimidinase (DHPase) structural analysis. (A) Diagrams of a fragment of the crystal structures of wild-type DHPase (left panel) and R118Q (right panel). R118 and Q118 are shown in yellow. (B) Diagrams of a fragment of the crystal structures of wild-type DHPase (left panel) and T418I (right panel). T418 and I418 are shown in yellow. (C) Diagrams of a fragment of the crystal structures of wild-type DHPase (left panel) and Y448H (right panel). Y448 and H448 are shown in yellow.

Tables

Table 1

DPYS variants previously identified in 3,554 Japanese subjects

| db SNP rsID | Location | Nucleotide change | Amino acid substitution | Frequency (%) | Effect | References |
|--------------|----------|-------------------|-------------------------|---------------|----------------------|--|
| rs199618701 | Exon 1 | 17G>A | R6Q | 0.11 | Increased | (Akai et al., 2015; Hishinuma et al., 2017) |
| rs572241599 | Exon 1 | 48C>G | N16K | 0.03 | No activity | (Yeung et al., 2013; Hishinuma et al., 2017) |
| rs1321466782 | Exon 1 | 175G>T | V59F | 0.01 | Unknown | - |
| rs1265124946 | Exon 1 | 241G>C | D81H | 0.02 | Unknown | - |
| rs371567511 | Exon 2 | 350G>A | W117X | 0.06 | No activity expected | - |
| rs368802826 | Exon 2 | 353G>A | R118Q | 0.01 | Unknown | - |
| rs755791096 | Exon 2 | 407C>T | T136M | 0.01 | Unknown | - |
| rs36027551 | Exon 3 | 541C>T | R181W | 2.86 | No effect | (Thomas et al., 2007; Hishinuma et al., 2017) |
| rs1181568837 | Exon 3 | 566C>T | A189V | 0.06 | Unknown | - |
| rs996605020 | Exon 5 | 884A>G | H295R | 0.01 | Unknown | - |
| rs121964923 | Exon 6 | 1001A>G | Q334R | 0.39 | Reduced | (Hamajima et al., 1998; Nakajima et al., 2016; Hishinuma et al., 2017) |
| rs771149650 | Exon 7 | 1093C>T | H365Y | 0.01 | Unknown | - |
| rs755440333 | Exon 7 | 1228G>A | G410S | 0.01 | Unknown | - |
| rs1401252393 | Exon 8 | 1253C>T | T418I | 0.01 | Unknown | - |
| - | Exon 8 | 1342T>C | Y448H | 0.04 | Unknown | - |
| rs201280871 | Exon 8 | 1393C>T | R465X | 0.03 | No activity | (van Kuilenburg et al., 2010; Hishinuma et al., 2017) |
| rs142574766 | Exon 9 | 1468C>T | R490C | 0.03 | No activity | (Hamajima et al., 1998; van Kuilenburg et al., 2010; Hishinuma et al., 2017) |
| rs189448963 | Exon 9 | 1469G>A | R490H | 0.07 | Unknown | - |
| - | Exon 9 | 1537A>G | T513A | 0.01 | Unknown | - |

Table 2

Polymerase chain reaction primers used in this study to amplify sequences of the human *DPYS* gene

| Nucleotide change | Primer (5'-3') | | Product length (bp) |
|-------------------|----------------------|----------------------|---------------------|
| | Sense | Antisense | |
| 175G>T | tgcaggagggcaccccaagc | gaggcggcctgctgaggac | 444 |
| 241G>C | | | |
| 353G>A | atgcccttctgggtcattta | tctgtcctctgtgtctag | 423 |
| 407C>T | | | |
| 566C>T | gagcagcagcagtttaccag | gccaatcatcttcacctta | 454 |
| 884A>G | | | |
| 1093C>T | tatctgtagggtttggag | gctcccttaccctaacct | 532 |
| 1228G>A | | | |
| 1253C>T | catcctcagatgctctacaa | ctacatcctctatgccaaga | 476 |
| 1342T>C | | | |
| 1469G>A | tcaagtgagctggtgatgat | ggaaatcccgaactgaccta | 489 |
| 1537A>G | | | |
| | cacaaaaagtgggacaatcc | gtgaagcctctgacctgat | 421 |

Table 3

Kinetic parameters of dihydropyrimidinase (DHPase) variants for dihydrouracil metabolism

| Variants | K_m (μM) | V_{max} (pmol/min/Unit) | CL_{int} (V_{max}/K_m) ($\mu\text{L}/\text{min}/\text{Unit}$) | % of Wild-type CL_{int} |
|----------|-------------------------|---------------------------|---|---------------------------|
| Wt | 8.32 ± 0.33 | 45.37 ± 0.64 | 5.45 ± 0.17 | 100.00 |
| R118Q | 8.86 ± 2.12 | 45.50 ± 2.93 | 5.27 ± 0.83 | 96.61 |
| A189V | 8.53 ± 2.07 | 49.23 ± 3.52 | 5.96 ± 1.20 | 109.34 |
| H295R | 4.30 ± 1.23 * | 2.12 ± 0.17 *** | 0.51 ± 0.11 *** | 9.42 |
| H365Y | 10.24 ± 1.14 | 62.92 ± 1.17 *** | 6.19 ± 0.63 | 113.51 |
| G410S | 8.06 ± 1.87 | 63.30 ± 2.25 *** | 8.19 ± 2.23 | 150.16 |
| T418I | 7.20 ± 2.10 | 34.91 ± 3.08 *** | 5.09 ± 1.27 | 93.40 |
| Y448H | 6.82 ± 1.45 | 29.99 ± 1.07 *** | 4.51 ± 0.77 | 82.60 |
| T513A | 6.44 ± 0.44 | 34.41 ± 0.85 *** | 5.35 ± 0.23 | 98.10 |

Data represent the mean \pm standard deviation of three independent catalytic assays. All assays and measurements were performed in triplicate using a single S-9 preparation. * $P < 0.05$, and *** $P < 0.005$ compared with wild-type (Wt) DHPase. The kinetic parameters of V59F, D81H, T136M, and R490H could not be determined because enzymatic activity was not detected at the highest substrate concentration used in the assay (300 μM dihydrouracil). K_m , Michaelis constant; V_{max} , maximum velocity; CL_{int} , intrinsic clearance.

Table 4

Kinetic parameters of dihydropyrimidinase (DHPase) variants for dihydro-5-fluorouracil metabolism

| Variants | K_m (μM) | V_{max} (pmol/min/Unit) | CL_{int} (V_{max}/K_m) ($\mu\text{L}/\text{min}/\text{Unit}$) | % of Wild-type CL_{int} |
|----------|-------------------------|---------------------------|---|---------------------------|
| Wt | 43.01 \pm 0.70 | 87.35 \pm 4.89 | 2.03 \pm 0.15 | 100.00 |
| R118Q | 39.36 \pm 6.82 | 56.82 \pm 3.63 *** | 1.46 \pm 0.17 *** | 71.98 |
| A189V | 29.94 \pm 2.44 | 66.98 \pm 2.38 *** | 2.24 \pm 0.15 | 110.45 |
| H295R | 107.28 \pm 23.14 | 11.02 \pm 1.40 *** | 0.10 \pm 0.01 *** | 5.12 |
| H365Y | 47.47 \pm 4.88 | 85.90 \pm 4.80 | 1.82 \pm 0.10 | 89.36 |
| G410S | 39.69 \pm 2.34 | 88.37 \pm 3.59 | 2.23 \pm 0.05 | 109.65 |
| T418I | 44.69 \pm 5.89 | 61.95 \pm 3.14 *** | 1.40 \pm 0.12 *** | 68.73 |
| Y448H | 39.54 \pm 1.70 | 53.59 \pm 1.14 *** | 1.36 \pm 0.05 *** | 66.74 |
| T513A | 40.70 \pm 3.18 | 54.48 \pm 1.73 *** | 1.34 \pm 0.07 *** | 66.05 |

Data represent the mean \pm standard deviation of three independent catalytic assays. All assays and measurements were performed in triplicate using a single S-9 preparation. *** $P < 0.005$ compared with wild-type (Wt) DHPase. The kinetic parameters of V59F, D81H, T136M, and R490H could not be determined because enzymatic activity was not detected at the highest substrate concentration used in the assay (300 μM dihydro-5-fluorouracil). K_m , Michaelis constant; V_{max} , maximum velocity; CL_{int} , intrinsic clearance.

Figure 1

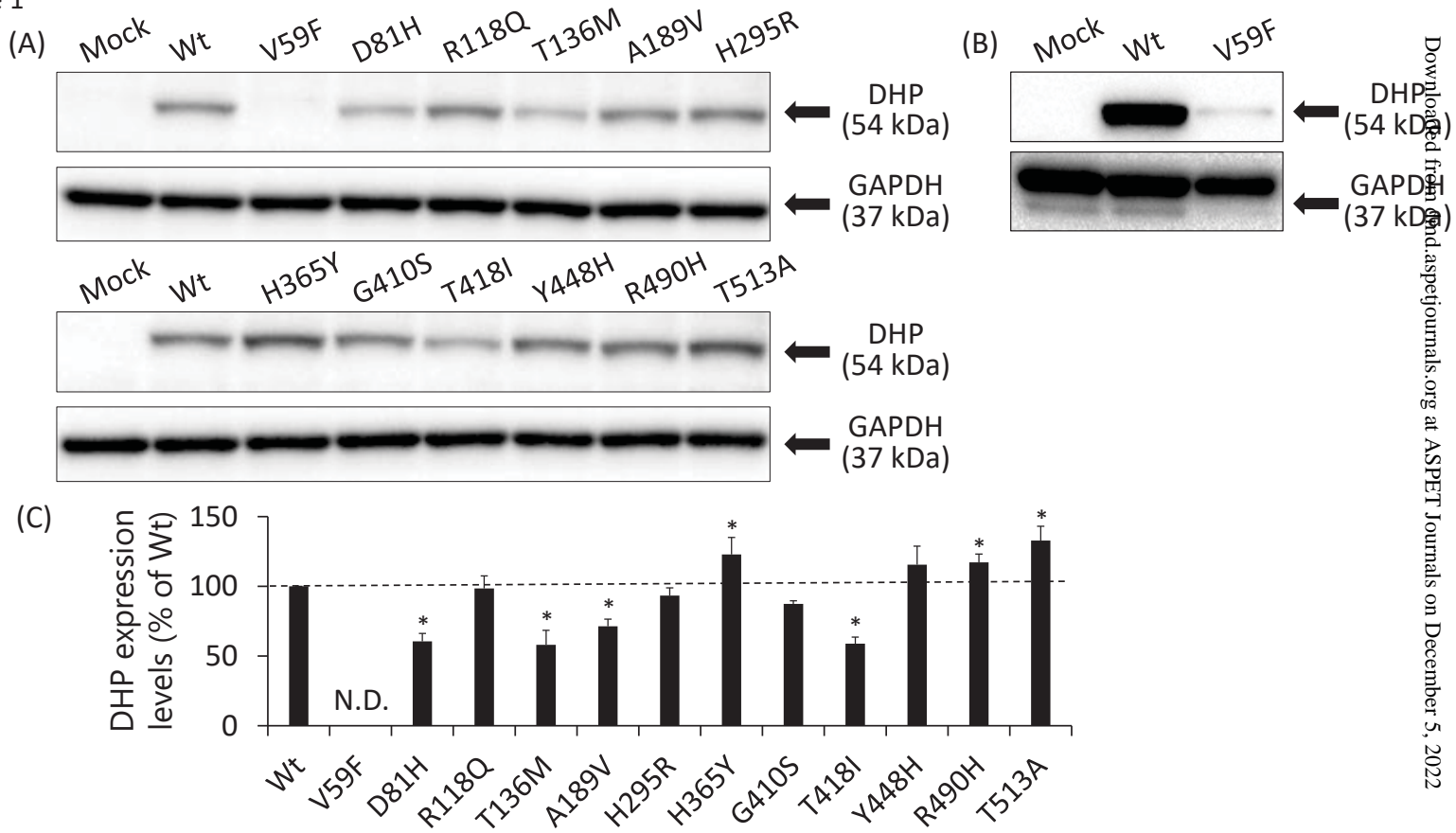


Figure 2

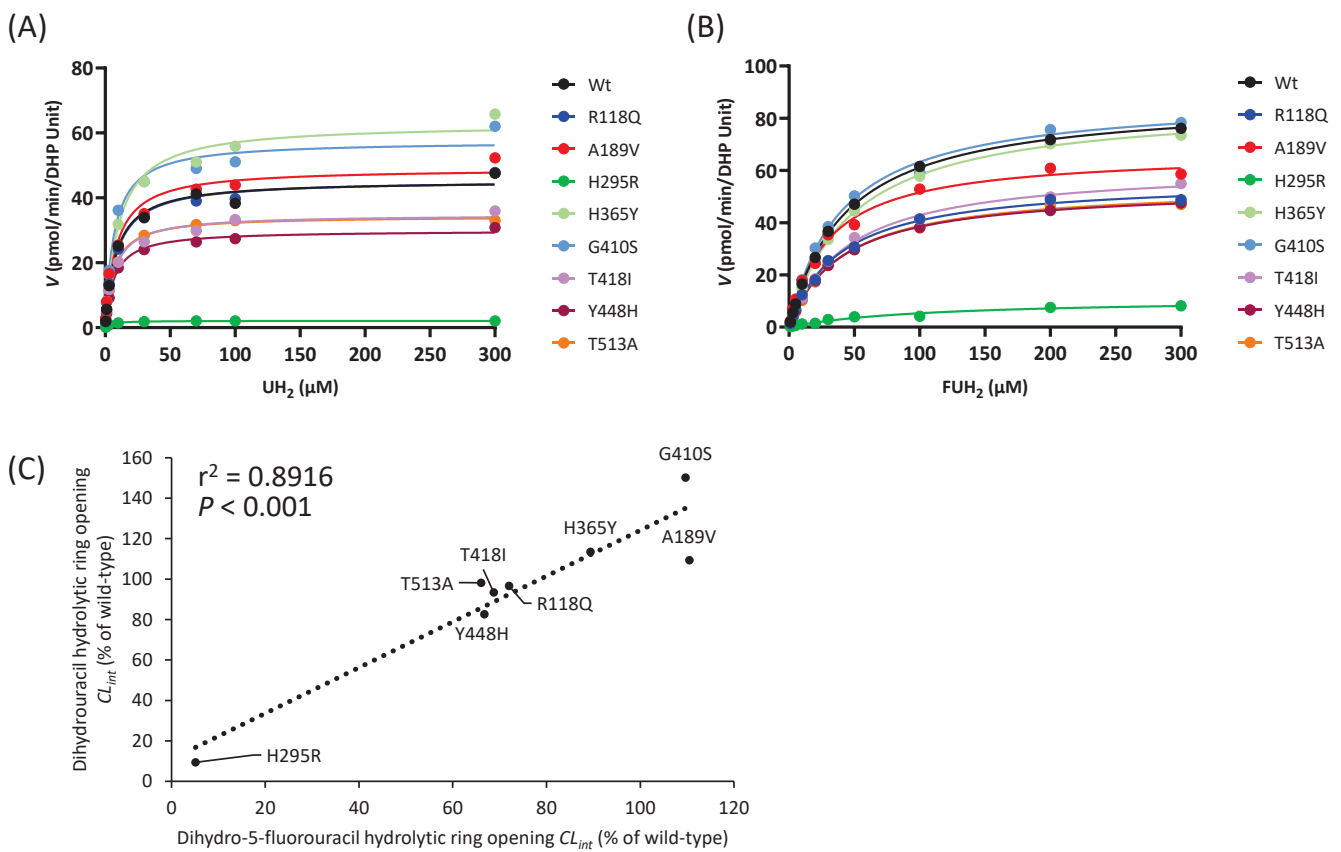


Figure 3

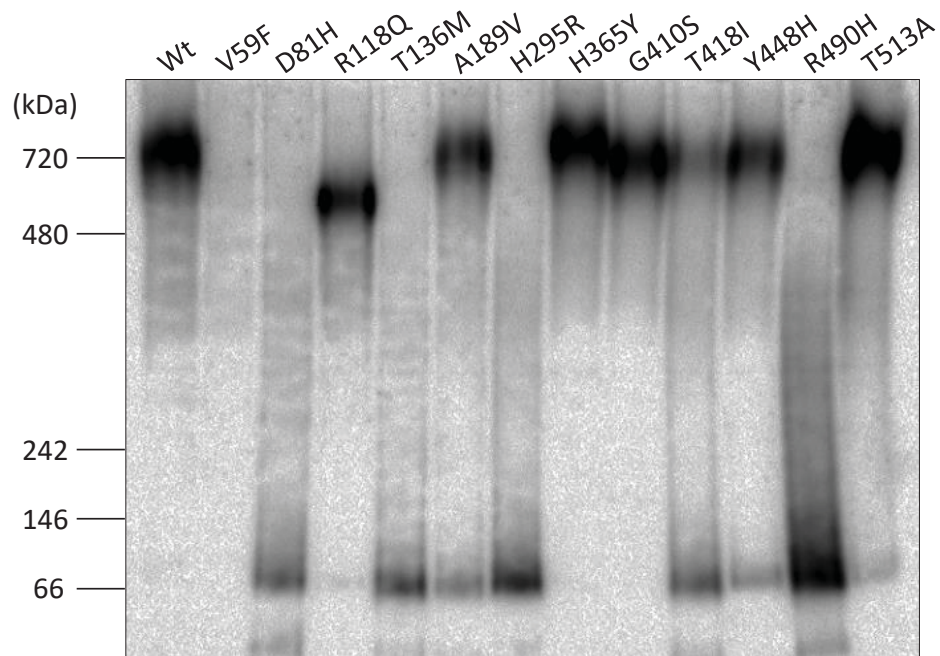


Figure 4

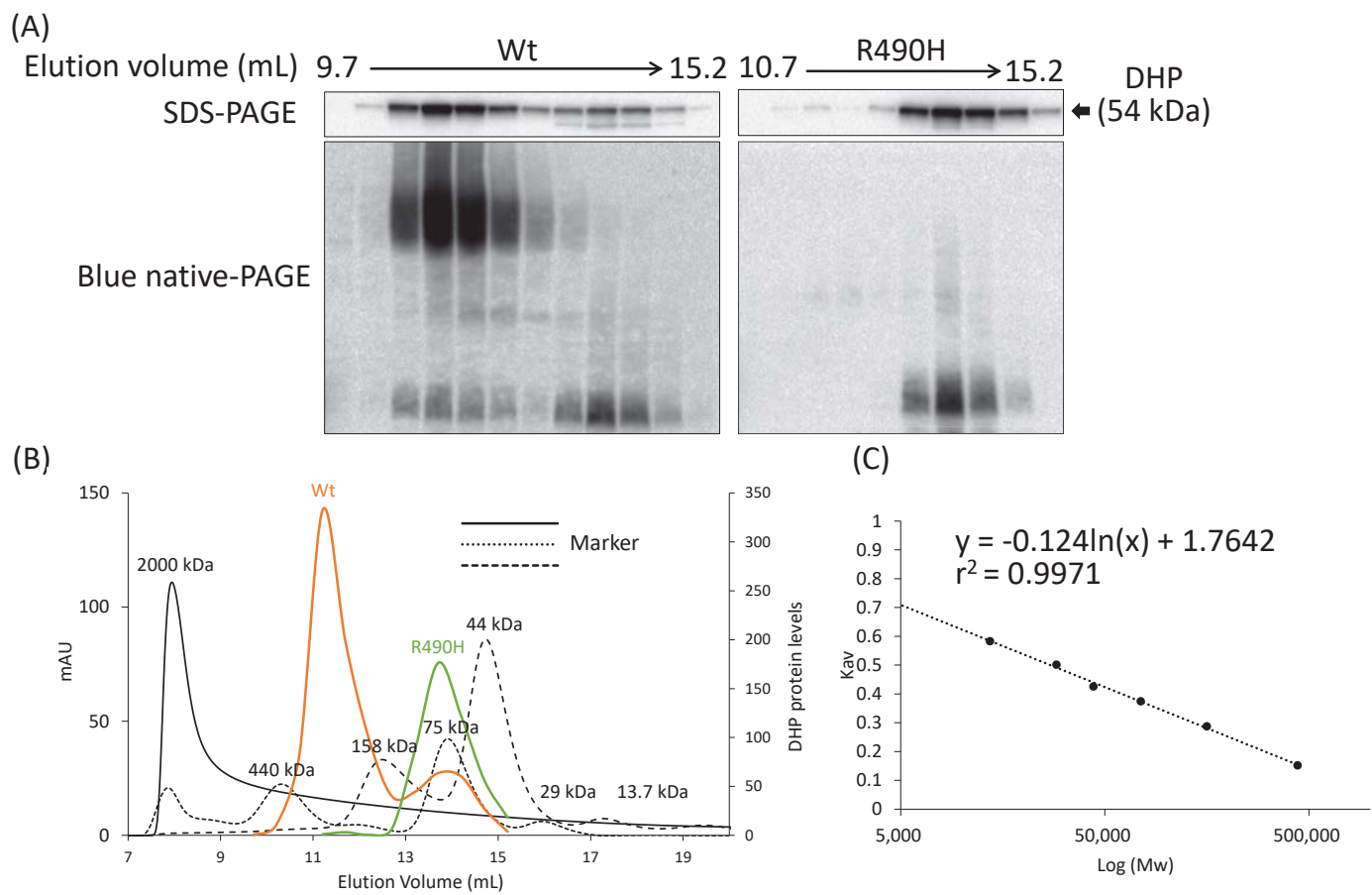


Figure 5

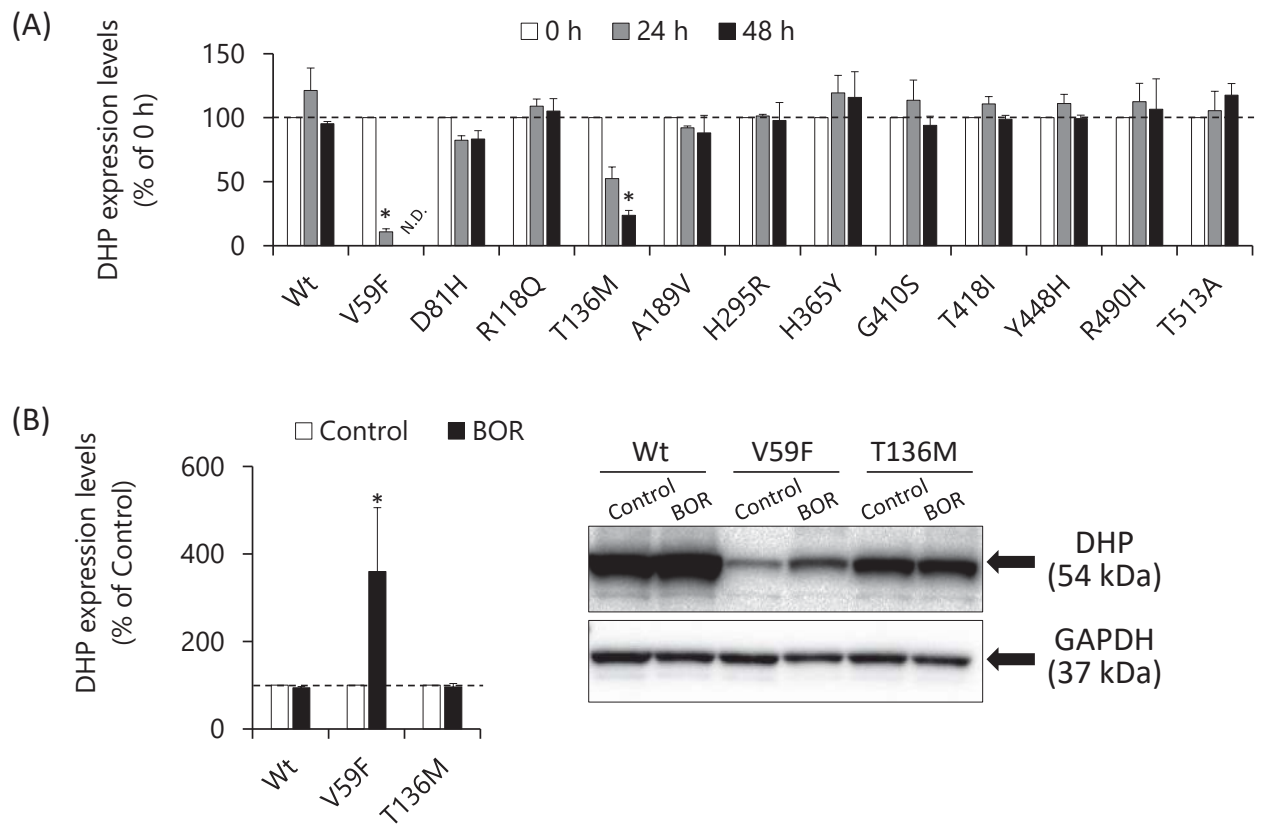


Figure 6

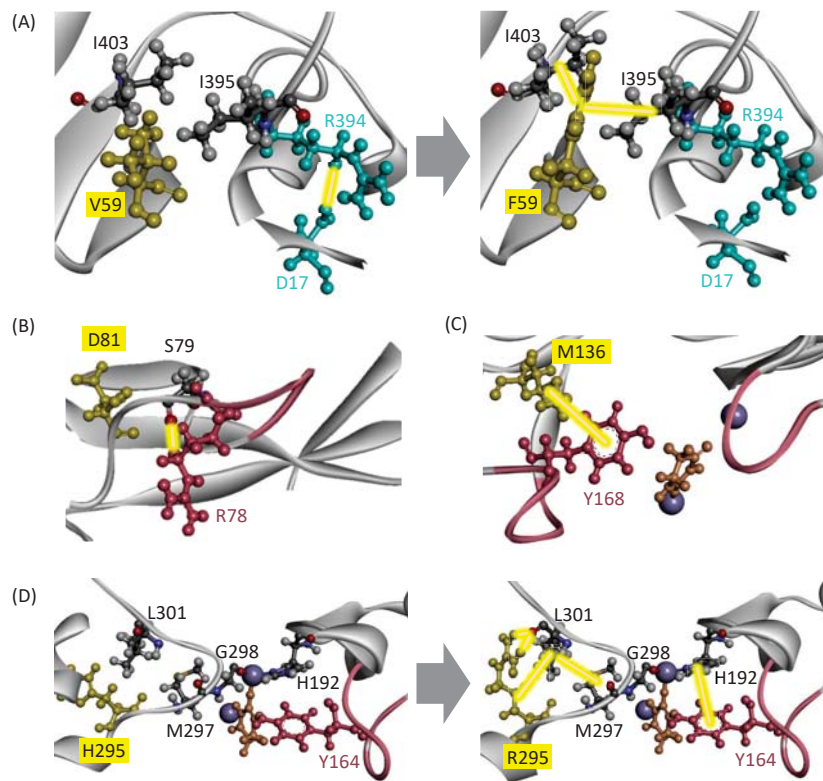


Figure 7

